Studies of granularity of a hadronic calorimeter for tens-of-TeV jets at a 100 TeV *pp* collider

S.V. Chekanov[a], M. Beydler[a], A.V. Kotwal[b,c], J. Proudfoot[a], S. Sen[b], N.V. Tran[c], S.-S. Yu[e], Chih-Hsiang Yeh[e]

[a] *HEP Division, Argonne National Laboratory, 9700 S. Cass Avenue, Argonne, IL 60439, USA.*
[b] *Department of Physics, Duke University, USA*
[c] *Fermi National Accelerator Laboratory*
[d] *Department of Physics, Michigan State University, 220 Trowbridge Road, East Lansing, MI 48824*
[e] *Department of Physics, National Central University, Chung-Li, Taoyuan City 32001, Taiwan*

Abstract

Texts

Keywords: multi-TeV physics, *pp* collider, future hadron colliders, FCC, SppC

1. Introduction

Particle collisions at energies beyond those attained at the LHC will lead to many challenges for detector technologies. Future experiments, such as high-energy LHC (HE-LHC), future circular *pp* colliders of the European initiative, FCC-hh [**?**] and the Chinese initiative, SppC [**?**].

The studies of this paper are based on full Geant4 simulation and reconstruction as implemented in the detector described in [**?**]. This study included the discussion of the impact of the calorimeter granularity on the shape of hadronic showers in terms of the calorimeter hits for two particles separated by some angle. It was concluded that HCAL granularity is essential in resolving two close-by particles for energies above 100 GeV. This paper makes a new step towards understanding of this problem using high-level physics quantities used in physics studies.

2. Studies of effective jet radius

The effective radius is the average of the energy weighted radial distance in $\eta - \phi$ space of jet constituents. Recently, it has been studied for multi-TeV jets in Ref.[**?**].

New we sill study jet splitting the effect of granularity on jet splitting scales. A jet k_T splitting scale [**?**] is defined as a distance measure used to form jets by the k_T recombination algorithm [**?** **?**]. This has been studied by ATLAS [**?**], and more

Email addresses: chekanov@anl.gov (S.V. Chekanov), mmbeydler@gmail.com (M. Beydler), ashutosh.kotwal@duke.edu (A.V. Kotwal), proudfoot@anl.gov (J. Proudfoot), sourav.sen@duke.edu (S. Sen), ntran@fnal.gov (N.V. Tran), syu@cern.ch (S.-S. Yu), a9510130375@gmail.com (Chih-Hsiang Yeh)

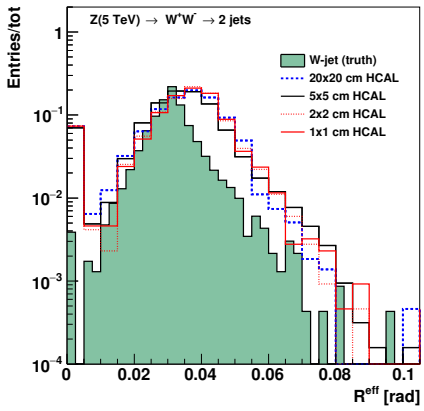

(a) 5 TeV

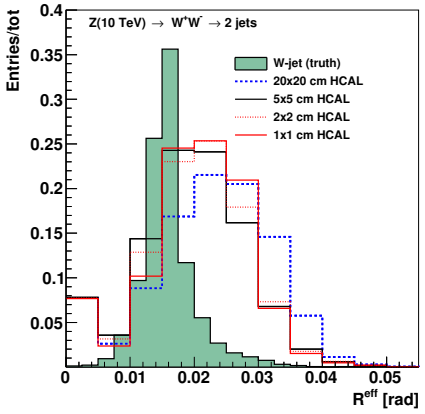

(b) 10 TeV

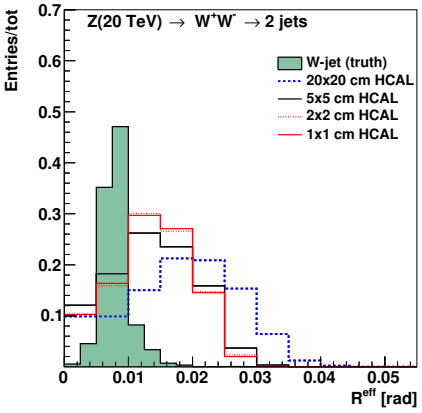

(c) 20 TeV

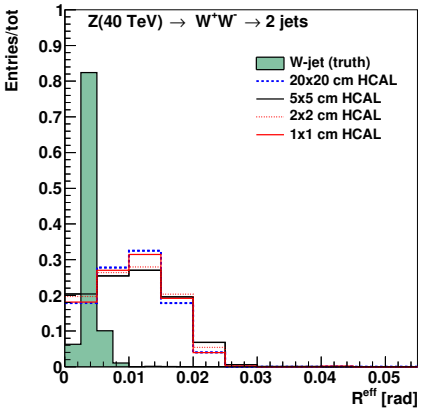

(d) 40 TeV

Figure 1: Jet effective radius for different jet transverse moment and HCAL granularity.

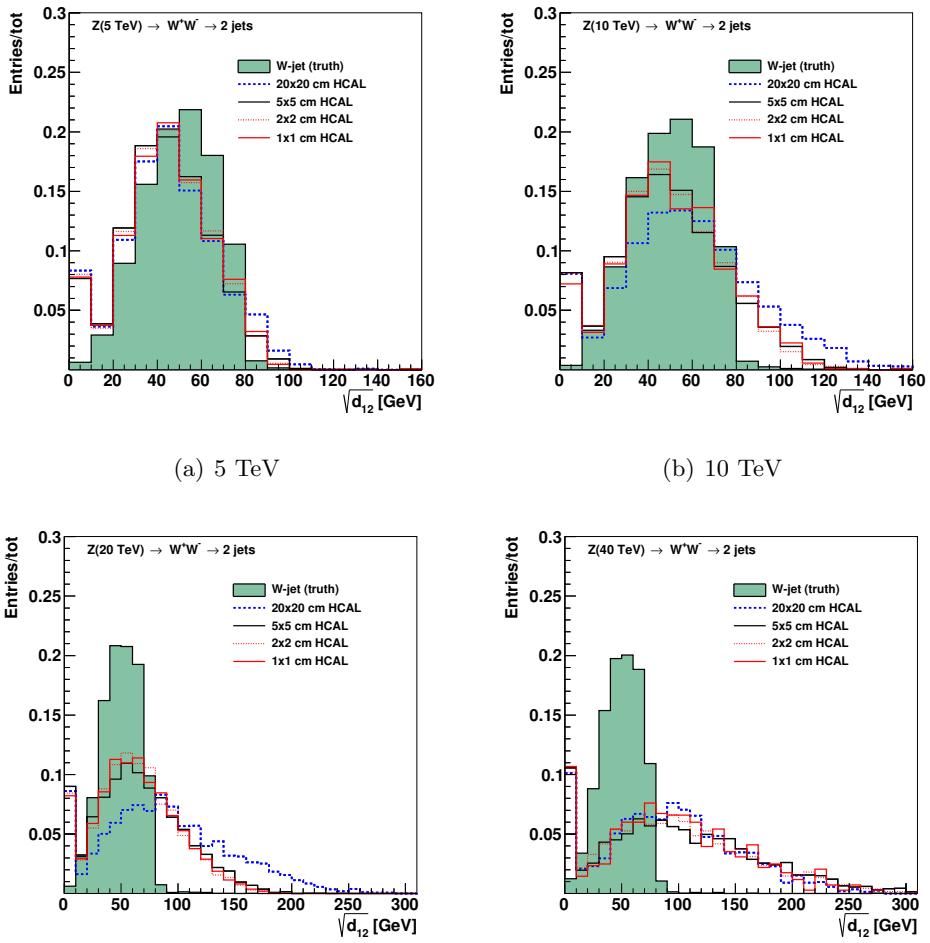

(a) 5 TeV

(b) 10 TeV

(c) 20 TeV

(d) 40 TeV

Figure 2: Jet splitting scale for different jet transverse moment and HCAL granularity.

recently in the context of 100 TeV physics [**?**]. The distribution of the splitting scale $\sqrt{d_{12}} = \min(p_T^1, p_T^2) \times \delta R_{12}$ [**?**] at the final stage of the k_T clustering, where two subjets are merged into the final one, is shown in Fig. 2.

3. Studies of signal and background separation in detector-level of cluster

In the future detector, when the luminosity is increased, the pileup is bigger, and it will be more difficult to distinguish the signal and the background. In this section, we want to study different variables and see their ability to separate the signal and the background in different detector sizes in the clustering of detector-level.

Figure 3 to 5 show the ROC curves of three variables, $c2b1$, τ_{21}, and τ_{32}. For each variable, there are three different sizes of the sub-detector HCAL compared at

four special collision energies. For different sizes, the one with the highest background rejection rate, which is 1-background efficiency, at the same signal efficiency has the best separate ability.

In Figure 3 for the variable $c2b1$, all ROC curves of the detector sizes are closed to each other for every cases of energy. So the the detector size is not sensitive to the separate ability in this variable.

For the tau21 variable in Figure 4, at 5 TeV, the smallest detector size (1×1 cm) can separate the background from the signal well. However, this is not the usual case as the ROC curves nearly merge together at higher collision energy. In addition, the detector with the bigger size tends to have higher separation ability than the smaller detector size in 20 and 40 TeV collision energy.

Figure 5 show variable τ_{32}, the smallest detector size has the best separate at all the cases of energy. This is what we want to see, because we want to use the smaller detector size to enhance the separation ability.

In conclusion,in all the cases of energy and detector size, the variable $c2b1$ has the better separation ability than the other two variables. In addition, the variable τ_{32} follows the rule that the smaller detector size has the better separation ability. We think this two variables could help to separate the signal and the background in the future detector analysis.

Acknowledgements

This research was performed using resources provided by the Open Science Grid, which is supported by the National Science Foundation and the U.S. Department of Energy's Office of Science. We gratefully acknowledge the computing resources provided on Blues, a high-performance computing cluster operated by the Laboratory Computing Resource Center at Argonne National Laboratory. Argonne National Laboratory's work was supported by the U.S. Department of Energy, Office of Science under contract DE-AC02-06CH11357. The Fermi National Accelerator Laboratory (Fermilab) is operated by Fermi Research Alliance, LLC under Contract No. DE-AC02-07CH11359 with the United States Department of Energy.

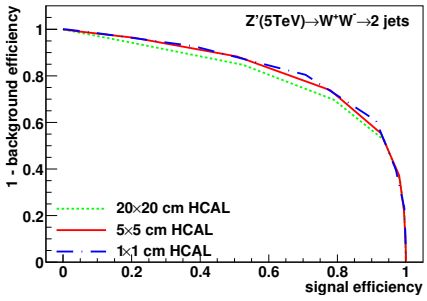

(a) 5 TeV

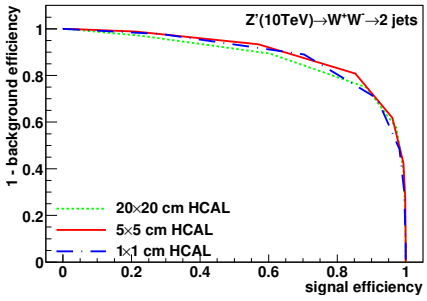

(b) 10 TeV

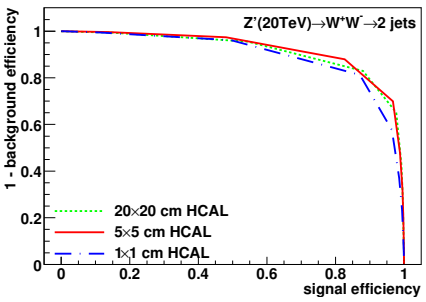

(c) 20 TeV

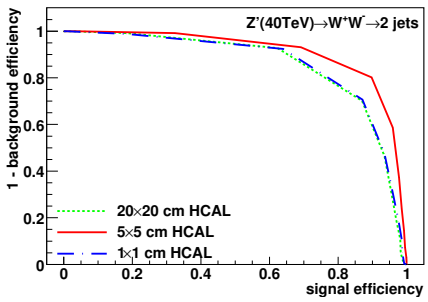

(d) 40 TeV

Figure 3: Signal efficiency versus background rejection rate using $c2b1$.The energies of collision at (a)5, (b)10, (c)20, (d)40TeV are shown here. In each picture of the energy, there are three ROC curves corresponding to different detector sizes.

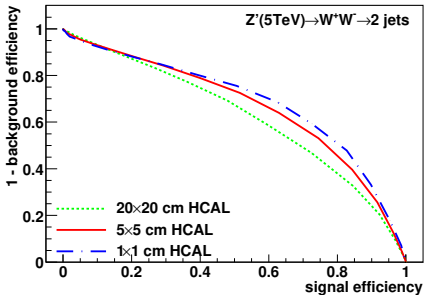

(a) 5 TeV

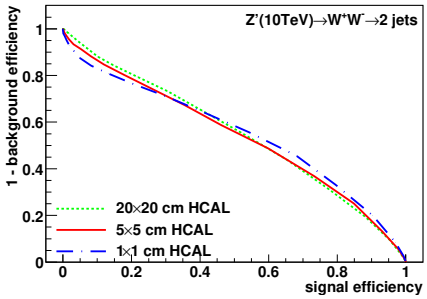

(b) 10 TeV

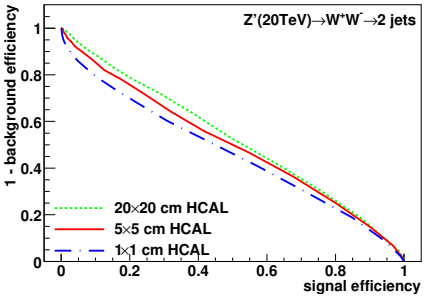

(c) 20 TeV

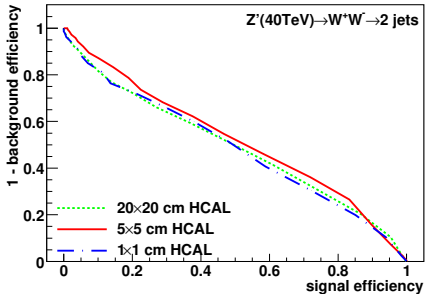

(d) 40 TeV

Figure 4: Signal efficiency versus background rejection rate using τ_{21}.The energies of collision at (a)5, (b)10, (c)20, (d)40TeV are shown here. In each picture of the energy, there are three ROC curves corresponding to different detector sizes.

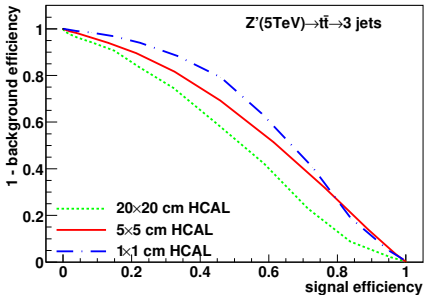

(a) 5 TeV

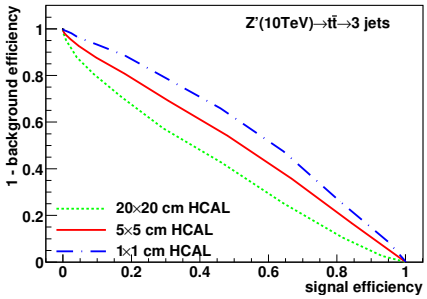

(b) 10 TeV

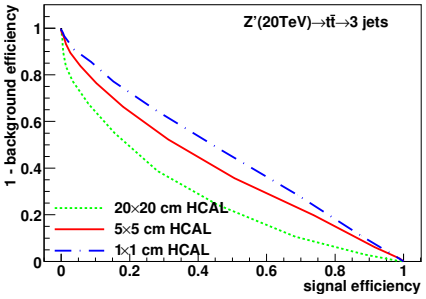

(c) 20 TeV

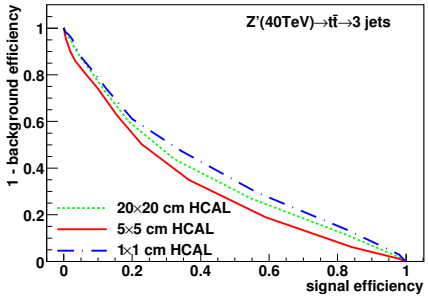

(d) 40 TeV

Figure 5: Signal efficiency versus background rejection rate using τ_{32}.The energies of collision at (a)5, (b)10, (c)20, (d)40TeV are shown here. In each picture of the energy, there are three ROC curves corresponding to different detector sizes.

References